Defense Technical Information Center
Compilation Part Notice

ADP013786

TITLE: Investigations of Optical Properties of Active Regions in Vertical Cavity Surface Emitting Lasers Grown by MBE

DISTRIBUTION: Approved for public release, distribution unlimited

This paper is part of the following report:

TITLE: THIN SOLID FILMS: An International Journal on the Science and Technology of Condensed Matter Films. Volume 412 Nos. 1-2, June 3, 2002. Proceedings of the Workshop on MBE and VPE Growth, Physics, Technology [4th], Held in Warsaw, Poland, on 24-28 September 2001

To order the complete compilation report, use: ADA412911

The component part is provided here to allow users access to individually authored sections of proceedings, annals, symposia, etc. However, the component should be considered within the context of the overall compilation report and not as a stand-alone technical report.

The following component part numbers comprise the compilation report:
ADP013771 thru ADP013789

Investigations of optical properties of active regions in vertical cavity surface emitting lasers grown by MBE

K. Regiński[a,*], T. Ochalski[a], J. Muszalski[a], M. Bugajski[a], J.P. Bergman[b], P.O. Holtz[b], B. Monemar[b]

[a]Department of Physics and Technology of Low Dimensional Structures, Institute of Electron Technology, 02-668 Warsaw, Poland
[b]Department of Physics and Measurement Technology, Linköping University, S-581 83 Linköping, Sweden

Abstract

The design of the vertical cavity surface emitting lasers (VCSELs) needs proper tuning of many different optical parameters of those structures. So, the optimisation of the VCSELs requires deep understanding of optical processes occurring in the active regions of such lasers. In a series of MBE processes, active regions of VCSELs as well as the whole VCSELs were grown. The active regions of the VCSEL structures were designed for $\lambda = 1000$ nm and 980 nm emission. They consisted of a pair of distributed Bragg reflectors (DBRs) composed of AlAs and GaAs quarter wavelength layers and a cavity made of GaAs. The cavities contained one or several quantum wells (QWs) made of $In_{0.2}Ga_{0.8}As$. To optimise the optical characteristics of the active regions, several experimental methods have been applied. The Bragg reflectors and the whole microcavities were investigated by optical reflectivity. For selective excitation of a QW in a cavity active layer, a Ti–sapphire tuneable laser has been used. The fine tuning between the QW emission and the cavity Fabry–Pérot resonance has been investigated by photoluminescence at varying temperatures of the sample. For monitoring the temporal evolution of the luminescence from the active region of the laser, time-resolved spectroscopy has been employed. The combination of many methods of optical investigations enabled a comprehensive characterisation and as a result an optimisation of the whole laser structure. © 2002 Elsevier Science B.V. All rights reserved.

Keywords: Molecular beam epitaxy; Planar microcavities; Vertical cavity surface emitting lasers

1. Introduction

Vertical cavity surface emitting lasers (VCSELs) have attracted much attention in recent years because of their potential for practical applications. VCSELs are also fascinating objects of fundamental studies as they have many dramatically different features in contrast with conventional semiconductor lasers. A variety of different devices have been demonstrated so far by using various growth techniques [1–3]. One of the frequently used methods of growing VCSELs is by molecular beam epitaxy (MBE).

The laser cavity of a VCSEL is usually constructed normal to the substrate plane by stacking multilayer films including an active region and two dielectric mirrors. Such a structure forms a Fabry–Pérot cavity resonator. A dielectric mirror can be formed with a periodic stack of quarter wavelength thick layers of alternating high and low refractive index material. Such

a mirror is referred to as a distributed Bragg reflector (DBR). The dielectric layers can be semiconductor layers deposited via MBE growth. The active region consists usually of a layer of GaAs of the thickness of one wavelength or two wavelengths and of one or several quantum wells (QWs) of InGaAs. (In our case $In_{0.20}Ga_{0.80}As$ has been applied.) The QWs are typically situated in the antinodes of a standing electromagnetic wave [4]. An example of such a structure is presented in Fig. 1, which shows the whole VCSEL structure designed for $\lambda = 1000$ nm emission. A 2λ-cavity is made of GaAs and contains 3×3 QWs made of $In_{0.20}Ga_{0.80}As$.

The procedure of designing the MBE process for growing the VCSEL structure comprises two classes of problems. The first one is connected with growing the materials of high quality for all parts of the structure. This optimisation concerns GaAs, Al(Ga)As, and InGaAs compounds. The problem is typical for MBE technology and can be solved by standard methods (see Regiński et al. [5]). The second group of problems is characteristic of the VCSEL structure. Optimisation of such a structure requires a precise tuning of its main

*Corresponding author. Institute of Electron Technology, 32/46 Al. Lotnikόw, PL-02-668 Warsaw, Poland. Tel.: +48-22-5487-920; fax: +48-22-8470-631.
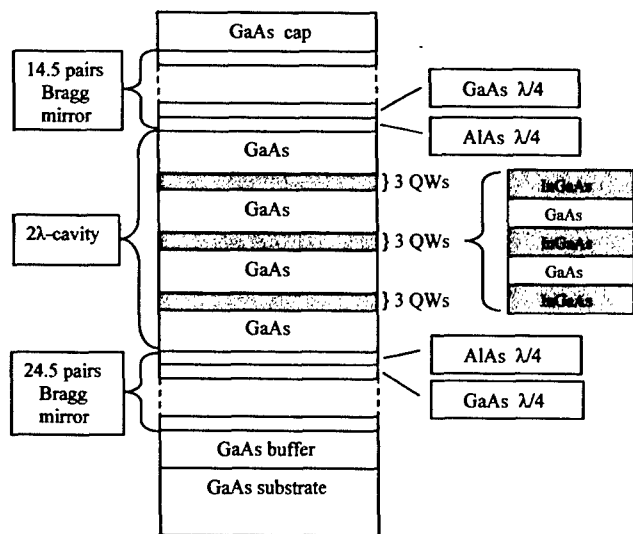*E-mail address:* reginski@ite.waw.pl (K. Regiński).

Fig. 1. Schematic VCSEL structure with 3×3 InGaAs QWs active region designed for $\lambda = 1000$ nm emission.

parts—DBRs, GaAs cavity, and QWs. This is the reason why the structure performance is very sensitive to variations in thickness of layers and their compositions. The wavelength of radiation from the QW depends on both the composition and thickness. The reflectivity of DBRs in the case of GaAs/AlAs reflectors depends on the layer thickness in the mirrors. Similarly, the position of the cavity resonance depends on the thickness of the spacer layers between the mirrors and the QWs region together with the phase of the reflection from the mirrors. Thus, the optimal growth of the structure requires simultaneous alignment of all three features. However, some variation of those parameters can be tolerated depending on how much variation in the threshold and efficiency is acceptable from device to device.

From the theoretical modelling as well as from the test processes it follows that the structure perfection is very sensitive to variation in thickness of the separate layers and their composition [4]. So the required accuracy can hardly be achieved without additional non-standard internal control in the MBE system. Thus, besides the careful calibration of the growth rate and composition, some non-standard methods of internal control should be applied. Moreover, to test the grown structures, we should combine several methods of post-growth characterisation. The most important one is the investigation of the optical properties of active regions. It comprises post-growth characterisation of separate DBRs, microcavities, and complete VCSEL structures. Naturally, the experimental work should be combined with theoretical calculations of the optical properties of the structures.

The goal of this paper is a demonstration how to combine different optical methods of post-growth char-

acterisation in order to optimise the VCSEL structures and to achieve precise control of MBE processes. We concentrate rather upon the methodology of measurements than on the detailed experimental results. Special emphasis is put on a time-resolved spectroscopy which is a non-standard technique rarely used for such applications (see Shah [8] and the literature therein). It allows us to study certain features of laser dynamics before producing the complete VCSEL structure, which is an element of novelty.

2. Design and growth of the structures

The structures investigated in this study were typical active regions of VCSELs. They consisted of cavity resonators with one or more quantum wells (QWs) situated in the antinodes of a standing electromagnetic wave. The thickness of the GaAs layer was typically one wavelength (λ-cavity) or two wavelengths (2λ-cavity). The DBRs were composed of semiconductor layers (AlAs and GaAs) and the QWs are of $In_{0.20}Ga_{0.80}As$. An example of such a structure containing 3×3 QWs is presented in Fig. 1. To the structure, for completeness, a cap layer is added, so in effect this is the whole VCSEL structure designed for $\lambda = 1000$ nm emission.

The growth processes reported in this study have been performed by the Elemental Source MBE technique on a RIBER 32P machine equipped with ABN 135L evaporation cells. The molecular fluxes were measured by a Bayard–Alpert gauge mounted on the sample manipulator. The manipulator could be rotated so as to place the Bayard–Alpert gauge at the standard position of the substrate. Thus the gauge could measure the beam equivalent pressure (BEP) of the As_4, Ga, Al and In beams.

For monitoring the state of the crystal surface during the growth, a reflection high-energy electron diffraction (RHEED) system with a 10-keV electron gun was used. The RHEED patterns were registered by a CCD camera and then processed in real time and recorded by a computer acquisition system. This system consists of a personal computer equipped with a frame grabber, two monitors, and a high-resolution laser printer. The RHEED pictures could be processed by a specially written computer program and stored on a hard disc. The system also enables us to register the RHEED intensity oscillations and, as a result, to determine the growth rate of a layer.

The substrate temperature was measured with a thermocouple and simultaneously with an IRCON Modline Plus pyrometer. This particular model of pyrometer is specially designed to measure the GaAs surface temperature by monitoring the radiation emitted in a narrow range of wavelengths (0.940 ± 0.03 μm) which is shorter than the band edge of GaAs (but longer than $Al_xGa_{1-x}As$, $x > 0.25$) at the temperatures which are of
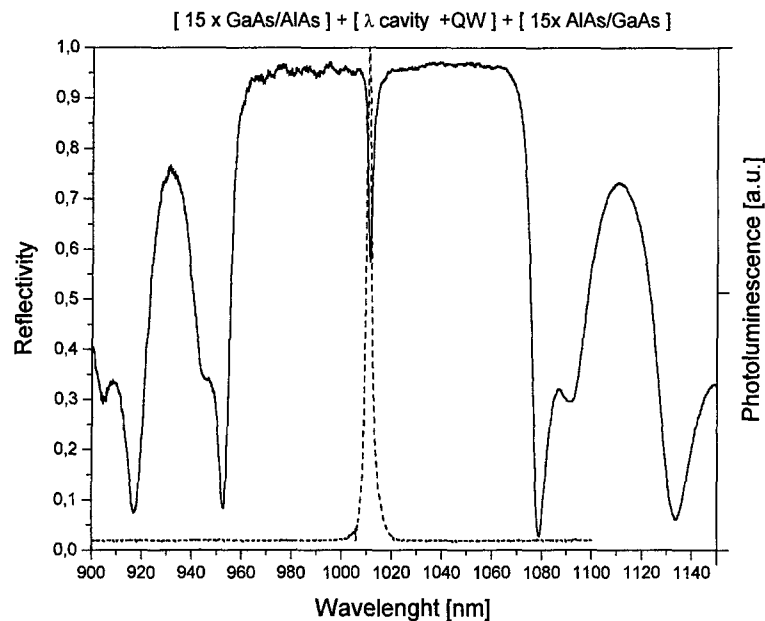
Fig. 2. Reflectance and photoluminescence spectra from the structure consisting of Bragg reflectors, λ-cavity, and $In_{0.2}Ga_{0.8}As$ QW.

interest for MBE (400–750 °C). The pyrometer is connected to a computer system enabling registration of the pyrometric temperature as a function of time. During the growth of the structure, even if the temperature registered by a thermocouple is constant, the pyrometric temperature oscillates in time. The source of those apparent temperature oscillations is the interference of the radiation emitted from the substrate and the radiation reflected at the underlying layer/grown layer and grown layer/vacuum interfaces. The phase information and the period of oscillations provide information on the actual growth rate, whereas the mean value of the pyrometer readout correlates with the true substrate temperature. Analysis of the oscillation curve after the growth gives a direct information about the thickness of all the layers in the grown structure. Thus, the interference pyrometry offers a convenient alternative to a standard laser reflectometry when it is necessary to control growth rate of layers with high precision.

The presented system enabled to control the growth rate of the individual layers with an accuracy of approximately 1%. More details about this control system can be found in [6]. The procedure of calibration of the growth process has been presented elsewhere [5].

The growth processes have been performed on heavily doped (p- or n-type) GaAs substrates of (001) orientation. Sometimes, for optical pumping experiments, the structures were undoped. The optimised growth temperatures were as follows: the GaAs:Be buffer layer was grown at 590 °C; the AlAs/GaAs Bragg reflectors, the GaAs cavities and the $In_{0.2}Ga_{0.8}As$ QWs were grown at a constant temperature 520 °C. The growth rate for GaAs and AlAs was 1 μm/h. The background pressure

during the growth was 5×10^{-8} torr. The whole process was performed without interruption. During the growth of the main structure, the substrate temperature shown by a thermocouple was kept constant. The pyrometer readouts demonstrated that this method of regulation leads to a really good thermal stabilisation of the substrate.

The grown structures were initially characterised by transmission electron microscopy (XTEM). It demonstrated that the interfaces between separate layers are sharp and the periodicity of the AlAs/GaAs layers is in a good accordance with the project. The interfaces between the QWs and the cavity as well as those between the cavity and the Bragg reflectors are strait and sharp. No defects of the structure are visible. This is a proof that the InGaAs layers are stressed and no misfit dislocations are generated. The detailed procedure of XTEM characterisation has been presented elsewhere [5].

3. Reflection and photoluminescence measurements

The process of optimising the technology comprised post-growth characterisation of the separate Bragg reflectors, the microcavities, and the complete VCSEL structures. Optical properties of the grown structures were investigated by optical reflectivity, photoluminescence, and time-resolved spectroscopy. The reflectivity spectra were measured in an experimental arrangement by using a halogen lamp as a source of incident white light. After reflection the relevant wavelength was selected by a monochromator and registered by a Ge detector. Fig. 2 shows a typical reflectance spectrum
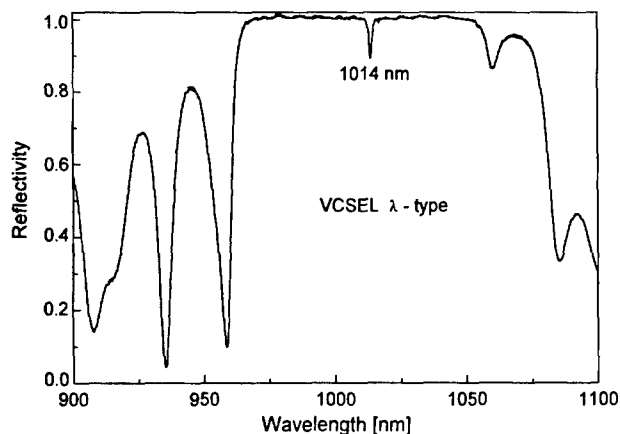
Fig. 3. Reflectance spectrum from a VCSEL of λ-type with an $In_{0.2}Ga_{0.8}As$ QW.

measured from the structure consisting of Bragg reflectors, λ-cavity and $In_{0.2}Ga_{0.8}As$ QW. A reflectance spectrum for the whole VCSEL structure is presented in Fig. 3. The measured spectra are similar to those calculated for ideal structures and exhibit the cavity resonance centred in the high reflectivity band of the Bragg reflectors. All the spectra exhibit broad stop bands, where the plot is almost flat. The reflectivity within those frequency intervals attains nearly 100%. The stop bands are bounded by deep minima which also testifies the good quality of the DBRs.

Photoluminescence (PL) measurements give us important information about the InGaAs quantum wells. To excite the quantum well, a Ti–sapphire tuneable laser has been used. Depending on the size of the cavity we observed either an enhancement or suppression of the coupling of 1e–1hh electronic dipole transitions into the resonant Fabry–Pérot mode of the planar microcavity structure.

The structures were excited with a laser beam perpendicular to their surface. The emission was recorded either from the edge of the structure (in plane photoluminescence) or in the direction perpendicular to its surface. The emission from the edge does not show any modifications (comparing with a separate QW) and can be treated as a reference. The emission from the surface shows the resonance with a Fabry–Pérot resonator. The large amplitude of this signal can be regarded as proof of good tuning between the wavelength emitted from the quantum well and the cavity resonance. An example of PL measurements is shown in Fig. 2. This figure shows a typical PL spectrum measured from the structure consisting of Bragg reflectors, λ-cavity and $In_{0.2}Ga_{0.8}As$ QW. The narrow PL peak corresponds to the case of good tuning.

The fine tuning between the QW emission and the cavity Fabry–Pérot resonance has also been investigated by PL for varying temperature of the sample. Even

when the whole system is not well tuned, we can test the structure by monitoring the luminescence as a function of temperature. By changing the temperature we can shift the frequency of the wave emitted from the QW and achieve the resonance for a certain temperature.

The perfection of the cavity is characterised by the quality factor Q (see Sale [4] for definition). In low-Q cavities the spontaneous emission from QWs can be described by the Fermi's golden rule and the system is classified to be in a weak coupling regime. In contrast, in high-Q semiconductor microcavities the exciton and photon interact coherently with each other forming a new eigenstate of the system called a cavity–polariton. The cavity–polariton can be considered as a two-dimensional version of exciton–polariton in bulk semiconductors [7]. In such a case the system is classified to be in a strong coupling regime. The energy difference between these two polariton modes at the exciton–cavity resonance is called the Rabi splitting. This splitting can be observed in reflection, transmission, absorption, or photoluminescence spectra. In the case of photoluminescence, under excitation above the exciton gap, the energy separation between the two peaks as well as their intensities depend on the detuning between the exciton and the cavity. This detuning can be regulated by changing the temperature of the sample. Such a type of photoluminescence measurements is presented in Fig. 4. The figure shows the luminescence spectra of the sample containing a 2λ-cavity made of GaAs with 3×3 QWs made of $In_{0.20}Ga_{0.80}As$. The wavelength used for excitation was 800 nm, i.e. the excitation was above the band-gap in GaAs. The measurements were carried out at variable sample temperature. At the temperatures of 90 K and 100 K, we can observe the Rabi splitting of the luminescence peak.
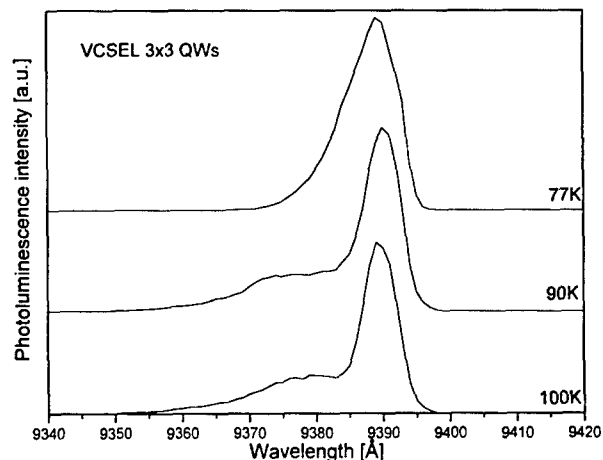

Fig. 4. Photoluminesence spectra of a VCSEL structure with 3×3 InGaAs QWs active region for variable temperature of the sample.

The precision requirements concerning the MBE processes are presented elsewhere [5]. The results presented above demonstrate good quality of grown structures, comparable with the results obtained by other authors (see Coldren et al. [3] and the literature therein). So, we can conclude that applying the presented methodology we can fulfil the assumed technological requirements.

The dynamical behaviour of the emission from cavity–polaritons depends on the way of excitation, i.e. the centre frequency and the bandwidth of the excitation light pulse. At resonant excitation, the type of response depends on whether only one or both of the two polariton modes are excited. When only one of the polariton modes is excited, the emission intensity from the microcavity decreases monotonously with time, since each polariton mode is an eigenstate of the system. When two modes are excited simultaneously, one can observe the mode oscillation, providing that the resolving power of the experimental set-up is sufficiently high.

In the case of non-resonant excitation, the excitons are created at an energy above the exciton gap. In this case, during the relaxation process, the phase coherence of the excitons is lost. Moreover, the excitons are distributed over a range of in-plane wavevector $k_\parallel$, where they couple to the 'open window modes'. The intensity of such modes is almost unchanged in comparison with those in free space. Therefore, under non-resonant excitation, the spontaneous emission characteristics in the strong coupling regime is not much different from that in the weak coupling regime. However, we can still observe the mode splitting.

The photoluminescence measurements presented above are also connected with time-resolved spectroscopy, which is the subject of Section 4.

4. Time-resolved spectroscopy

The time-resolved spectroscopy enables us to study many important features of the active region of the laser, such as the time of increasing of the spontaneous emission after the excitation, the decay time of the exciton population, the threshold of lasing action, etc. [8]. These features are connected directly with the perfection of the microcavity (characterised by the quality factor Q) and its tuning to the oscillators (QWs).

The dynamics of the luminescence after excitation is mainly determined by relaxation processes in the exciton population. Thus, the time-resolved spectroscopy enables us to investigate the relaxation processes of the excitons. The thermalisation and relaxation time of the excitons is determined primarily by exciton–acoustic phonon and the exciton–exciton interactions. The second mechanism depends strongly on the density of excitons and dominates for high densities.
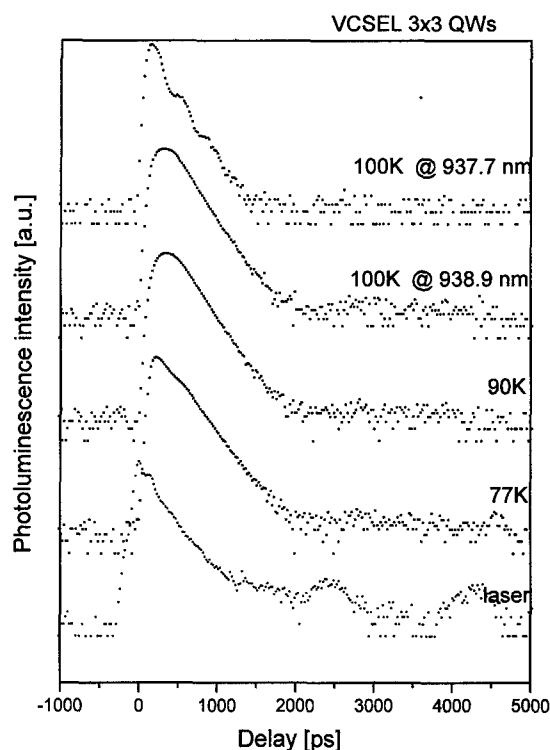

Fig. 5. Emission decay for an optically pumped VCSEL structure with 3×3 InGaAs QWs active region for variable temperature of the sample. Experimental points are presented on a semi-logarithmic scale and displaced vertically for clarity.

To measure time-resolved luminescence spectra, a standard experimental set-up has been employed. It consisted of a pulsed laser generating the exciting pulses, a photomultiplier as a detector and time-to-amplitude conversion electronics. The laser pulse width was 100 fs and the temporal resolution of the whole experimental arrangement was approximately 50 ps. The wavelength used for excitation was 800 nm, i.e. the excitation was above the band-gap of GaAs. The set-up enabled us to carry out the measurements at variable sample temperature starting from 77 K until ambient temperature and for different pulse energy.

All the time-resolved measurements presented below were carried out on the sample containing a 2λ-cavity made of GaAs with 3×3 QWs made of $In_{0.20}Ga_{0.80}As$.

As it was mentioned in the previous section, in the case of non-resonant excitation in the strong coupling regime we observe the characteristic Rabi splitting in the luminescence spectra. In such a case, we can monitor time-resolved luminescence spectra corresponding to either peak. An example of such measurements is presented in Fig. 5. The main luminescence peak is attributed to the wavelength of 938.9 nm and the secondary one to 937.7 nm. The measurements have been performed for variable temperature of the sample and at very low pulse energy of the excitation. This
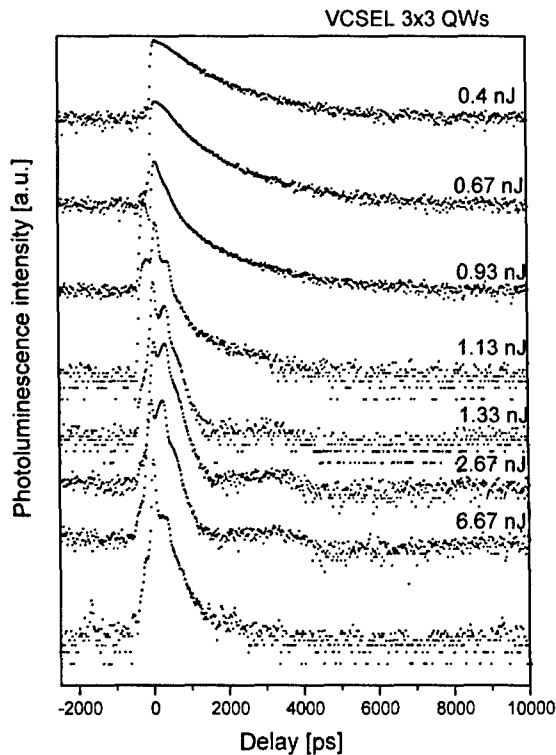
Fig. 6. Emission decay for an optically pumped VCSEL structure with 3×3 InGaAs QWs active region at 77 K for variable pumping pulse energy. Experimental points are presented on a semi-logarithmic scale and displaced vertically for clarity.

type of measurement confirms the nature of both the luminescence peaks.

In what follows in this section, we will restrict ourselves to the temperature of 77 K and the investigation of the dynamics of the main peak.

Shown in Fig. 6 are the examples of temporal behaviour of the emission intensity from the active region of VCSEL for different excitation densities. It is well visible that the luminescence intensity increases faster at higher excitation densities. As it was expected, higher density of excitons increases exciton–exciton interaction and hence the rate of thermalisation of excitons. The decrease of intensity at each decay curve shows a simple exponential form. Such a behaviour is qualitatively similar to the case of bare QW excitons in the strong coupling regime. This part of the curve is dominated by the population dynamics of the incoherent excitons distributed over a wide range of $k_{\parallel}$ and in the different spin states. Therefore, the excitons can couple to the 'open window modes' and radiate photons similarly to the case of bare QWs. The 'splitting' of the uppermost part of the decay curves is caused by a complicated shape of the exciting pulse, which is composed of a main pulse followed by a secondary pulse.

Another important feature shown in Fig. 6 is connected with a threshold of lasing action. When the pulse
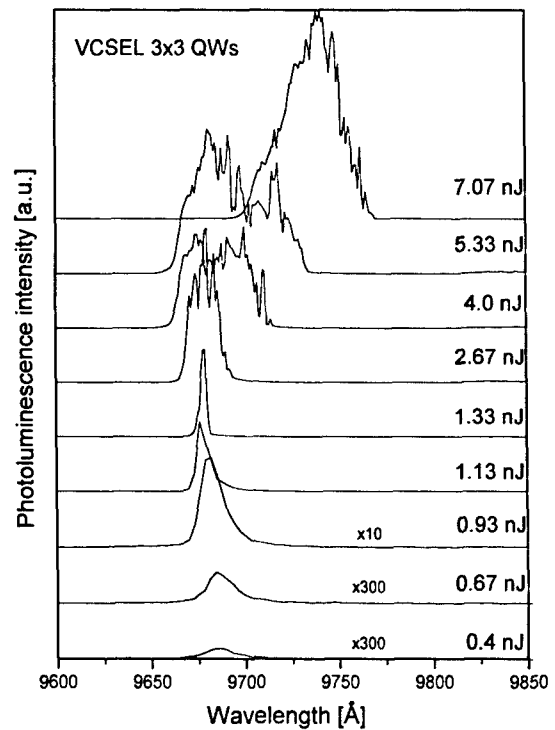

Fig. 7. Photoluminesence spectra of a VCSEL structure with 3×3 InGaAs QWs active region for variable pumping pulse energy.

energy is greater than 1.13 nJ, the form of the decay curves changes rapidly. First, the decay time is much shorter than that for weaker excitations. Next, the height of the two split peaks is almost equal, which shows saturation of the luminescence. These results correlate well with those presented in Fig. 7 where the luminescence from the active region is presented as a function of pulse energy of the exciting laser. It is evident that above 1.13 nJ, both the amplitude and the shape of the luminescence spectra change rapidly. The shape of the
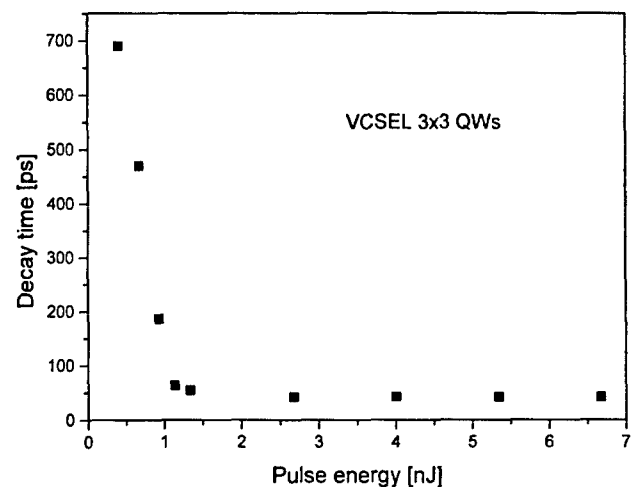

Fig. 8. Carrier lifetime vs. pumping pulse energy for a VCSEL structure with 3×3 InGaAs QWs active region.

spectra does not represent properly the lasing modes of the laser because of instability of the investigated system. Nevertheless, certain characteristic features of the mode structure are well visible. Moreover, the peak amplitude for excitations above 1.13 nJ is two orders of magnitude higher than that for the lower excitations.

The dependence of the decay time on the pulse energy of the excitation is shown in Fig. 8. It is well demonstrated that above 1.13 nJ, this time does not decrease with increasing energy. It confirms our claim that this energy corresponds to the threshold of lasing action. Additionally, this plot enables us to estimate the temporal resolution of the experimental set-up to approximately 50 ps.

5. Conclusions

We have presented several optical methods of post-growth characterisation of the active regions of VCSELs grown by MBE. The optical properties of grown structures were investigated by optical reflectivity, photoluminescence, and time-resolved spectroscopy. The investigations comprised optical characterisation of the separate Bragg reflectors, the microcavities, and the complete VCSEL structures. Combining the selected methods we were able to estimate in detail the quality of the DBRs and the microcavities as well as the tuning of the quantum wells to the microcavities. Optical methods also enabled us to estimate whether the system works in a strong coupling regime. Finally, we could

investigate in detail the threshold of the lasing action. Thus, by using the above-described methods, we could optimise the construction of the VCSEL structures. Moreover, we have achieved a very precise ex situ control of the MBE processes.

References

[1] T. Baba, T. Hamano, F. Koyama, K. Iga, Spontaneous emission factor of a microcavity DBR surface emitting laser, IEEE J. Quantum Electron. 27 (1991) 1347.

[2] C.J. Chang-Hasnain, Vertical-cavity surface-emitting lasers, in: G.P. Agrawal (Ed.), Semiconductor Lasers; Past, Present, and Future, AIP Press, Woodbury, 1995, pp. 145–180.

[3] L.A. Coldren, E.R. Hegblom, Y.A. Akulova, J. Ko, E.M. Strzelecka, S.Y. Hu, VCSELs in 98: What we have and what we can expect, in: K.D. Choquette, R.A. Morgan (Eds.), Vertical-Cavity Surface-Emitting Lasers II, Proceedings of SPIE, vol. 3286, pp. 2–16.

[4] T.E. Sale, Vertical Cavity Surface Emitting Lasers, Research Studies Press, Taunton, 1995, p. 55.

[5] K. Regiński, J. Muszalski, M. Bugajski, T. Ochalski, J.M. Kubica, M. Zbroszczyk, J. Kątcki, J. Ratajczak, MBE growth of planar microcavities with distributed Bragg reflectors, Thin Solid Films 367 (2000) 290–294.

[6] J. Muszalski, Pyrometric interferometry during MBE growth of laser heterostructures, Thin Solid Films 367 (2000) 299–301.

[7] Y. Kadoya, Microcavity effects in semiconductor quantum wells, in: T. Ogawa, Y. Kanemitsu (Eds.), Optical Properties of Low-Dimensional Materials, World Scientific, Singapore, 1998.

[8] J. Shah, Ultrafast Spectroscopy of Semiconductors and Semiconductor Nanostructures, Springer, Berlin, Heidelberg, New York, 1999.